HHS Public Access

Author manuscript

World J Urol. Author manuscript; available in PMC 2016 August 01.

Published in final edited form as:

World J Urol. 2015 August ; 33(8): 1119–1128. doi:10.1007/s00345-014-1403-5.

Temporal expression of hyaluronic acid and hyaluronic acid receptors in a porcine small intestinal submucosa-augmented rat bladder regeneration model

Fadee G. Mondalek[1,2], **Kar-Ming Fung**[1,3,4], **Qing Yang**[1], **Weijuan Wu**[1,5], **Wenli Lu**[1,6], **Blake W. Palmer**[1], **Dominic C. Frimberger**[1], **Beverley Greenwood-Van Meerveld**[4,5,7], **Robert E. Hurst**[1,8], **Bradley P. Kropp**[1], and **Huesh-Kung Lin**[1,3]

[1]Department of Urology, University of Oklahoma Health Sciences Center, Oklahoma City, OK 73104, USA

[2]Department of Chemical, Biological & Materials Engineering, University of Oklahoma, Norman, OK 73019, USA

[3]Department of Pathology, University of Oklahoma Health Sciences Center, Oklahoma City, OK 73104, USA

[4]Oklahoma City Department of Veterans Affairs Medical Center, Oklahoma City, OK 73104, USA

[5]Department of Physiology, University of Oklahoma Health Sciences Center, Oklahoma City, OK 73104, USA

[6]Department of Pediatrics, Shanghai Ruijin Hospital, Medical School of Shanghai Jiao Tong University, Shanghai 200025, China

[7]Oklahoma Center for Neuroscience, Oklahoma City, Oklahoma, 73104, USA

[8]Department of Biochemistry and Molecular Biology, University of Oklahoma Health Sciences Center, Oklahoma City, OK 73104

Abstract

Introduction—Hyaluronic acid (HA), a non-sulfated glycosaminoglycan, is an essential component of the extracellular matrix (ECM). Since HA is involved in many phases of wound healing and may play a key role in tissue repair and regeneration, this study was intended to understand temporal and spatial expression of HA and HA receptors (HARs) during the course of bladder regeneration in rats.

Materials and methods—Sprague-Dawley rats were subjected to partial cystectomy followed by augmentation with porcine small intestinal submucosal (SIS) prepared from distal sections of the small intestine. SIS-augmented bladders were harvested between post-operative days 2 and 56.

Results—Bladder regeneration proceeded without complications. All augmented bladders had complete urothelial lining and smooth muscle bundles by day 56 post-augmentation. Temporal

Address all correspondence and requests for reprints to: H. K. Lin, PhD., Department of Urology, University of Oklahoma Health Sciences Center, 920 Stanton L. Young Blvd., WP3150, Oklahoma City, OK 73104, Tel: (405) 271-6900, FAX: (405) 271-3118, hk-lin@ouhsc.edu.

and spatial distributions of HA and HARs were studied by immunohistochemistry in regenerating bladders. The strongest HA immunoreactivity was observed in the ECM on post-operative days 28 and 56. CD44 immunoreactivity was detected in the cytoplasm of urothelial cells on day 56; and LYVE-1 immunoreactivity was exclusively limited to lymphatic vessels on days 28 and 56.

Conclusions—We demonstrated that HA was synthesized throughout the course of bladder wound healing and regeneration; and HA deposition coincided with urothelial differentiation. Expression of CD44 and LYVE-1 followed the same temporal pattern as HA deposition. Therapeutic modalities through local delivery of exogenous HA to improve the outcome of SIS-mediated bladder regeneration might need to be coordinated with HAR expression in order to achieve maximal regenerative responses as opposed to fibrosis.

Keywords

hyaluronic acid; CD44; LYVE-1; wound healing; bladder regeneration

INTRODUCTION

Hyaluronic acid (hyaluronan; HA), a non-sulfated glycosaminoglycan (GAG), is an integral part of the extracellular matrix (ECM). HA is a polymer of disaccharides consisting of D-glucuronic acid and D-N-acetylglucosamine *via* alternating β-1,4 and β-1,3 glycosidic bonds. Sizes of the polymer can be from 5,000 to 20,000,000 Da *in vivo* depending upon the number of the disaccharide repeats. For example, averages of HA molecular weights are between $3–4\times10^6$ Da in human synovial fluid and human umbilical cord [1,2]. HA mediates a wide range of cellular activities from migration, proliferation, differentiation, morphogenesis, inflammation, and angiogenesis to cell-cell interactions and cell-ECM adhesions [3]. HA may, therefore, modulate a variety of cellular responses in various aspects of tissue repair and regeneration, such as new blood vessel formation [4]. Wound matrix is rich in HA in scarless fetal wound healing; and topical application of HA is associated with reduced scar formation in postnatal wounds [5].

HA-mediated biological activity is initiated by binding to and activating HA receptors (HARs). Several HARs have been identified including CD44, LYVE-1 (lymphatic vessel endothelial receptor 1), HARE (HAR for endocytosis), and RHAMM (receptor for HA mediated motility). CD44 is the major receptor for HA, and is widely expressed in epithelial, mesenchymal, and lymphoid cells in nearly all tissues [6]. CD44 plays an important role in HA-mediated physiology from cell aggregation, migration, proliferation, and activation, to cell-substrate and cell-cell interactions. LYVE-1 binds to both soluble and immobilized HA, and specifically localizes on the luminal face of lymphatic endothelial cells wall [6]. HARE, originally cloned from rat liver sinusoidal endothelial cells, is distinct from CD44 [7]. RHAMM is associated with locomotion of various cell types including migrating fibroblasts in wound healing, endothelial cell angiogenesis, and cancer cell metastasis [8,9].

Tissue engineering technology is intended to replace aplastic, hypoplastic, or pathologic tissues, and restore functionality of organs. HA has been incorporated into biomaterial designs [10] to modulate inflammatory responses [11], enhance cell differentiation [12], and improve vascularization [13]. In bladder reconstruction animal models, HA also has been

incorporated into scaffolds to improve the outcome of regeneration. To obtain the maximal benefits from exogenous HA, temporal change and spatial distribution of endogenous HA and HARs during the course of regeneration need to be defined. In this communication, we reported deposition of HA and expression of HARs in rat bladders following augmentation with porcine small intestinal submucosa (SIS).

MATERIALS AND METHODS

Preparation of porcine SIS

SIS was prepared from the distal segment of ileum obtained from a 3-year old sow. The tunica mucosa and the serosa muscularis were first mechanically removed as we described [14]. Any region that contains Peyer's patches was discarded. SIS membranes were sterilized by exposing to 0.1% peracetic acid (Sigma-Aldrich Inc.; St. Louis, MO) for 1 hour, washed three times with sterile distilled water for 5 min each, and stored in sterile water at 4 °C unitl use. SIS prepared in this manner provided consistent and reliable regeneration results [15].

Surgical procedures for bladder augmentation in rats

This study was approved by the Institutional Animal Care and Use Committee (IACUC) at the University of Oklahoma Health Sciences Center (OUHSC). Female Sprague-Dawley rats (250–300 g) were obtained from Charles River Laboratories (Raleigh, NC), and housed in the university animal care facility with standard light/dark cycles and free access to food and water. Animals were subjected to partial (40–50%) cystectomy followed by augmentation with 1×1 cm^2 pieces of distal porcine SIS as we reported [14]. Permanent sutures were placed for identification between SIS grafts and native bladders at harvest. Three rats were used in each time point in the experimental group. Three additional rats were subjected to partial cystectomy without SIS augmentation and used as a control. Bladder specimens obtained from partial cystectomy were used as normal bladder control.

Tissue collection and processing

At harvest, rats were euthanized with a lethal dose of pentobarbital between post-operative days 2 and 56. The bladder was inflated and fixed with 10% formalin, divided by a midline longitudinal incision, and embedded in paraffin. Paraffin sections were cut at 5 μm and mounted on glass slides, baked at 65 °C for 30 min, and stored at room temperature until use.

For RNA isolation, SIS grafts were separated from native bladders based on positions of permanent sutures between days 2 and 28 post-augmentation. Total RNA was extracted from SIS grafts, as well as native and normal bladders using Trizol® reagent. Isolated total RNA samples were quantified and stored in liquid nitrogen until use.

Immunohistochemical analysis

For histological evaluation, formalin-fixed paraffin-embedded (FFPE) bladder sections were stained with hematoxylin and eosin (H&E) using an automatic Tissue-Tek DRS 2000 slide stainer (Sakura, Torrance, CA). For immunohistochemical staining, bladder sections were deparaffinized in xylene, rehydrated in a series of graded alcohol followed by rinses with

0.01 M Tris-buffered saline (TBS). Sections were incubated with 0.5% H_2O_2 in TBS to eliminate endogenous peroxidase activity, followed by incubation with TBS containing 10% goat serum and 1% bovine serum albumin (BSA) for 2 hours to block non-specific binding. For HA staining, bladder sections were incubated with 5 μg/ml biotinylated HA binding protein (HABP; Sigma-Aldrich Inc.; St. Louis, MO) for 2 hours followed by rinses with TBS and incubation with 1:400 streptavidin-streptavidin-conjugated horseradish peroxidase (HRP; Vector Laboratories Inc.; Burlingame, CA) for another 2 hours at room temperature. HABP binding was visualized by incubating the sections with fast red substrate (BioGenex; San Ramon, CA). The slides were counterstained with hematoxylin (Anapath Inc.; Lewisville, TX), rinsed in tap water, and mounted with an aqueous mounting media.

Immunohistochemistry was applied to detect cytokeratin and HARs expression in regenerating rat bladders. Briefly, bladder sections were incubated with mouse anti-pan cytokeratin monoclonal antibody (1:1,000 dilution; Abcam; Cambridge, MA), mouse anti-rat CD44 antibody (1:400 dilution; Chemicon International; Temecula, CA), rabbit anti-human LYVE-1 antibody (1:800 dilution; Abcam), goat anti-human RHAMM antibody (1:400 dilution; Santa Cruz; Santa Cruz, CA), or mouse anti-rat HARE monoclonal antibody (1:2,000 dilution; provided by Dr. Paul Weigel, OUHSC) in TBS containing 1% BSA. A separate set of slides was incubated with the TBS diluent without primary antibody and used as a negative control. Following TBS rinses, bladder sections were incubated with 1:400 dilution of biotinylated horse anti-rat (CD44), biotinylated goat anti-rabbit (LYVE-1), biotinylated rabbit anti-goat (RHAMM), or biotinylated horse anti-mouse (cytokeratin and HARE) secondary antibody for 2 hours. After TBS washes, streptavidin-HRP (1:400 dilution in TBS and 1% BSA) was added and incubated for 30 min followed by TBS rinses. Bound antibodies were visualized by incubating with stable diaminobenzidine (DAB; Life Technologies; Carlsbad, CA) for 4 min; and color development was terminated by washing the slides with tap water. Tissue sections were counterstained with hematoxylin, rinsed in tap water, dehydrated in graded alcohol, cleared in xylene, and mounted with cover slips. Microscopic images were captured with a Nikon Eclipse 80i microscope (Melville, NY).

Quantification of LYVE-1-positive lymphatic vessels

To quantify numbers of lymphatic vessels in bladder tissues, LYVE-1 immunoreactive vessels were counted blindly in the regenerative, native, and normal sections. Results were expressed as mean ± standard deviation (SD) of numbers of LYVE-1-positive vessels/mm^2 from 3 animals in each time point.

Expression of HARs mRNA

Semi-quantitative RT-PCR was conducted to expression of HARE and RHAMM mRNAs. First-strand cDNA was synthesized from 1 μg of total RNA in the presence of 1 μg oligo $(dT)_{12–18}$ primers (Life Technologies) and 200 U Moloney murine leukemia virus (MMLV) reverse transcriptase in a total of 50 μl at 42 C for 2 hours. HARE and RHAMM were amplified from 1 μl of the first-strand cDNA in the presence of 0.2 μM each of forward and reverse primers, 200 μM dNTP, and 5 U *Taq* DNA polymerase (Life Technologies) in a total of 50 μl. PCR was titrated between 20 and 40 cycles for linear amplification of each mRNA target. Primer pairs, amplification conditions, and sizes of amplified products are described

in Supplementary Table S1. Aliquots (10 μl) of the amplified products were separated on 1% agarose gels. Images of ethidium bromide-stained gels were captured using Gel Doc 1000 (Bio-Rad Laboratories; Hercules, CA).

RESULTS

Morphology of SIS-augmented bladder regeneration

Compared to normal bladders (Figure 1A), at 2 days post-augmentation SIS scaffolds were absent of inflammatory cells or regenerating activity (Figure 1B). Chronic inflammatory cell infiltration was observed at earlier stages of regeneration on post-augmentation days 7 and 14 (Figure1C and 1D), but completely subsided from day 28 (Figure1E and 1F). Urothelium regeneration was noted in day 7 (Figure 1C). The urothelium appeared thickened during the mid regenerative stage (day 28) but returned to normal thickness on day 56 (Figure1E and 1F). Thickening of the urothelium appeared to be from larger sizes of individual epithelial cells rather than more numbers of cell layers. Organized smooth muscle bundles were observed from days 28 to 56.

Re-epithelialization of regenerating rat bladders

Cytokeratins are specific markers of epithelial cell differentiation. Normal rat bladders showed AE1/AE3-positive cytoplasmic staining in all layers of the urothelium (Figure 2A). AE1/AE3-positive staining was correlated with all phases of re-epithelialization from post-augmentation days 7 to 56 (Figure 2C–2F).

Temporal and spatial deposition of HA

Spatial deposition of HA was studied through a high affinity binding protein (HABP) using an immunohistochemistry-like method. To demonstrate HABP binding specificity, sections of normal bladders were pre-treated with hyaluronidase followed by HABP incubation. Negative immunoreactivity was observed after hyaluronidase digestion (Figure 3F). Minimal HABP binding activity was detected up to post-operative day 14 (Figure 3A–3C), whereas significant increases in HABP binding signals were observed from days 28 to 56 after augmentation (Figure 3D–3E). HABP binding was mainly localized to the ECM of stromal layers but not the urothelium.

CD44 and LYVE-1 expression

Changes in CD44 and LYVE-1 expression and their relationships with HA deposition were determined by immunohistochemistry.

CD44—CD44-positive immunoreactivity was minimal between days 2 and 14 post-augmentation (Figure 4A–4C). CD44 immunoreactivity was detectable, but limited to the urothelium on post-operative day 28 (Figure 4D); and staining intensity increased significantly by day 56 (Figure 4E). In contrast to HA deposition, no significant immunoreactivity was observed in stromal cells or the ECM. Strong CD44-posiitve immunoreactivity was also detected in lymphocytes in both grafts and native bladders adjacent to SIS (data not shown).

LYVE-I—Similar to CD44, LYVE-1-positive immunoreactivity was not detectable until post-operative day 28 (data not shown). LYVE-1-positive staining was limited to lymphatic vessels; and strong LYVE-1 immunoreactivity was detected in both graft and native regions of SIS-augmented bladders (Figure 5A). Quantification of LYVE-1-positive lymphatic vessels showed that normal bladders had 3.44 ± 0.06 lymph vessels/mm^2. In graft portions of augmented bladders, lymphangiogeneis reached 2.78 ± 1.56 and 1.95 ± 1.23 lymph vessels/mm^2 at post-operative days 28 and 56, respectively (Figure 5B). Numbers of lymphatic vessels between normal and regenerating bladders were not statistically significant on days 28 and 56 post-augmentation based on student's *t*-test.

RHAMM and HARE mRNA expression

HARE—HARE-positivity immunoreactivity was extremely weak, or absent, in normal and regenerating bladders at all time points (data not shown). HARE mRNA was barely detectible even after 40 cycles of PCR amplification from normal and regenerating bladders (Figure 6A), whereas the liver which was used as a positive control showed high levels of HARE mRNA expression using the identical PCR protocol (data not shown). Levels of HARE mRNA expression did not vary significantly during the course of SIS-augmented bladder regeneration (Figure 6B).

RHAMM—Commercial antibodies against RHAMM failed to demonstrate proper staining specificity in rat bladder tissue sections. Results from semi-quantitative RT-PCR demonstrated that steady increase in RHAMM mRNA was observed following SIS augmentation (Figure 6A). Normalized levels of RHAMM mRNA were significantly up-regulated within 2 days post-augmentation and remained elevated at day 28 in SIS graft sections (Figure 6B).

DISCUSSION

HA and HARs are involved in a variety of biological activities and tightly associated with wound repair and tissue regeneration. In this communication, accumulation of HA and expression of HARs were described in a SIS-augmented rat bladder regeneration model. HA was detected specifically in the ECM of stroma in graft regions of regenerating bladders prior to post-operative 28 days, but did not return to the level observed in the normal bladder at day 56. Similar to other reports, HA was identified in the connective tissue around smooth muscle fibers of rat bladders during wound healing and regeneration [16]. However, HA accumulation may be different depending on types of injuries and organs, or species of animals. For example, HA was detectable within 1 day after mucosal wounds in human cases [17]. HA was found to reach the maximal level between 7 and 14 days after radial keratotomy, and return to the normal level in 60 days in rabbit cornea and aqueous [18].

HA acts as a promoter and modulator of inflammation and other cellular responses in wound healing. HA enhances cellular infiltration and stimulates pro-inflammatory cytokines expression [19]. HA can also function as a negative regulator in inflammatory activation and protector of cells against free-radical damages [20]. HA-modulated cell proliferation and migration through direct interactions with HARs are important for proper tissue remodeling

and regeneration [21], and for promoting angiogenesis and lymphangiogenesis [13] in several regeneration models.

Similar to temporal changes in HA accumulation, CD44-positive staining was detected in both normal and regenerating bladders. In contrast, CD44 expression was limited to the cytoplasm of urothelial cells. Other studies described that CD44 is preferentially localized to epithelial cells of various organs specifically in regions with active cell growth, such as in the basal layers of stratified epithelium and at the base of the crypts of Lieberkuhn of the intestine [22]. Similar to our results, CD44 and HA are detected in separate anatomical locations. For example, CD44 is detected in the epidermis, whereas HA is localized to the dermis of the skin. In addition, CD44 is localized to the epithelial lining, whereas HA is prominently accumulated in the lamina propria in the intestine [22]. In contrast to our results, Oksala et al. reported that HA is detected in the wound margin and the connective tissue matrix, and co-localized with CD44-positive migrating keratinocytes in healing mucosa wound of the human skin [17].

HA and CD44 may respond to barrier injury and be involved in restoration of barrier function. Disruption of the stratum corneum leads to a marked accumulation of HA in the matrix between epidermal basal and spinous keratinocytes in a mouse model [23]. Although re-epithelialization occurs before terminal urothelium differentiation based on immunohistochemical studies, temporal changes of CD44 expression coincide with differentiation of urothelial cells and establishment of urine impermeability with uroplakin and ZO-1 expression [24]. In contrast to the expression of uroplakin in different layers of the urothelium and homogenous expression of ZO-1 during the course of regeneration processes, strong CD44 immunireactivity is present toward deeper layers of the urothelium at later stages of bladder regeneration. Similar patterns of CD44 expression have also been observed in epithelial cell differentiation during the development of taste buds [25] as well as keratinocyte differentiation and permeability barrier homeostasis in the skin [26]. In a transgenic mouse model with defective HA accumulation or CD44 expression, morphological alteration of basal keratinocytes, defective proliferation of keratinocyte in response to mitogens and growth factors, decrease in skin elasticity, impaired local inflammatory responses, and impaired tissue repair have been observed [27]. Rapid restoration of impermeable urothelium is particularly critical following bladder reconstruction to ensure proper regeneration processes. Paralleled HA accumulation and CD44 expression following bladder augmentation suggest these two molecules may work interactively in bladder regeneration. However, spatial distributions between HA and CD44 in regenerating bladders suggest that biological interactions between these two molecules require further studies.

LYVE-1 is exclusively expressed in lymphatic endothelial cells in regenerating rat bladders. Similar to temporal patterns of HA and CD44 expression, LYVE-1 was not detected until post-operative day 28. LYVE-1 expression can be regulated by pro-inflammatory cytokines. In bladder regeneration, expression of LYVE-1 increases as most of the inflammation receded [14]. In contrast to temporal expression of LYVE-1 in regenerating bladders, levels of vascular endothelial growth factor receptor (VEGFR)-3, another receptor involved in lymphangiogenesis, mRNA expression was significantly elevated within 2 days post-

augmentation (data not shown). RHAMM has been implicated in cell locomotion by activating intracellular protein kinases, i.e. extracellular signal-regulated protein kinase (ERK), p125fak, and pp60c-src [28]. Up-regulation of RHAMM mRNA may reflect its involvement in inflammatory cell infiltration during bladder regeneration.

Based on the importance of biological properties of HA, exogenous HA has been included in the design and fabrication of various biological scaffolds for wound healing and tissue repair. In surgical bladder reconstruction models, incorporation of HA into bladder accelular matrix enhances urothelial and smooth muscle cell migration and improve the outcome of regeneration [29]. We also demonstrated that inclusion of HA into porcine SIS enhanced angiogenesis of regenerative dog bladders [13]. Incorporation of HA into biomaterials can be a viable approach for urinary bladder regeneration by reducing scarring and improving completeness of regeneration.

CONCLUSIONS

Temporal changes in HA deposition and major HARs expression coincide with each other during the course of SIS-augmented rat bladder regeneration. Results from this report serve as a baseline for future design and incorporation of exogenous HA into biomaterials to modulate HARs expression in various cell types and to enhance complete and functional bladder regeneration.

Supplementary Material

Refer to Web version on PubMed Central for supplementary material.

Acknowledgments

This work was supported by a P20 research grant awarded by the National Institute of Diabetes and Digestive and Kidney Diseases (NIDDK, 5P20DK097799-02).

REFERENCES

1. Saari H, Konttinen YT. Determination of synovial fluid hyaluronate concentration and polymerisation by high performance liquid chromatography. Ann Rheum Dis. 1989; 48(7):565–570. [PubMed: 2774697]
2. Saari H, Konttinen YT, Friman C, Sorsa T. Differential effects of reactive oxygen species on native synovial fluid and purified human umbilical cord hyaluronate. Inflammation. 1993; 17(4):403–415. [PubMed: 8406685]
3. Reitinger S, Lepperdinger G. Hyaluronan, a ready choice to fuel regeneration: a mini-review. Gerontology. 2013; 59(1):71–76. [PubMed: 23006468]
4. Mondalek FG, Ashley RA, Roth CC, Kibar Y, Shakir N, Ihnat MA, Fung KM, Grady BP, Kropp BP, Lin HK. Enhanced angiogenesis of modified porcine small intestinal submucosa with hyaluronic acid-poly(lactide-co-glycolide) nanoparticles: From fabrication to preclinical validation. J Biomed Mater Res A. 2010; 94(3):712–719. [PubMed: 20213816]
5. Siebert JW, Burd AR, McCarthy JG, Weinzweig J, Ehrlich HP. Fetal wound healing: a biochemical study of scarless healing. Plast Reconstr Surg. 1990; 85(4):495–502. [PubMed: 2315389]
6. Banerji S, Ni J, Wang SX, Clasper S, Su J, Tammi R, Jones M, Jackson DG. LYVE-1, a new homologue of the CD44 glycoprotein, is a lymph-specific receptor for hyaluronan. J Cell Biol. 1999; 144(4):789–801. [PubMed: 10037799]

7. Zhou B, Weigel JA, Fauss L, Weigel PH. Identification of the hyaluronan receptor for endocytosis (HARE). J Biol Chem. 2000; 275(48):37733–37741. [PubMed: 10952975]
8. Park D, Kim Y, Kim H, Kim K, Lee YS, Choe J, Hahn JH, Lee H, Jeon J, Choi C, Kim YM, Jeoung D. Hyaluronic acid promotes angiogenesis by inducing RHAMM-TGFβ receptor interaction via CD44-PKCδ. Mol Cells. 2012; 33(6):563–574. [PubMed: 22610405]
9. Rein DT, Roehrig K, Schondorf T, Lazar A, Fleisch M, Niederacher D, Bender HG, Dall P. Expression of the hyaluronan receptor RHAMM in endometrial carcinomas suggests a role in tumour progression and metastasis. J Cancer Res Clin Oncol. 2003; 129(3):161–164. [PubMed: 12712331]
10. Li H, Chen C, Zhang S, Jiang J, Tao H, Xu J, Sun J, Zhong W, Chen S. The use of layer by layer self-assembled coatings of hyaluronic acid and cationized gelatin to improve the biocompatibility of poly(ethylene terephthalate) artificial ligaments for reconstruction of the anterior cruciate ligament. Acta Biomater. 2012; 8(11):4007–4019. [PubMed: 22813848]
11. Kajahn J, Franz S, Rueckert E, Forstreuter I, Hintze V, Moeller S, Simon JC. Artificial extracellular matrices composed of collagen I and high sulfated hyaluronan modulate monocyte to macrophage differentiation under conditions of sterile inflammation. Biomatter. 2012; 2(4):226–273. [PubMed: 23507888]
12. Mothe AJ, Tam RY, Zahir T, Tator CH, Shoichet MS. Repair of the injured spinal cord by transplantation of neural stem cells in a hyaluronan-based hydrogel. Biomaterials. 2013; 34(15): 3775–3783. [PubMed: 23465486]
13. Roth CC, Mondalek FG, Kibar Y, Ashley RA, Bell CH, Califano JA, Madihally SV, Frimberger D, Lin HK, Kropp BP. Bladder regeneration in a canine model using hyaluronic acid-poly(lactic-co-glycolic-acid) nanoparticle modified porcine small intestinal submucosa. BJU Int. 2011; 108(1): 148–155. [PubMed: 20942834]
14. Ashley RA, Palmer BW, Schultz AD, Woodson BW, Roth CC, Routh JC, Fung KM, Frimberger D, Lin HK, Kropp B. Leukocyte inflammatory response in a rat urinary bladder regeneration model using porcine small intestinal submucosa scaffold. Tissue Eng Part A. 2009; 15(11):3241–3246. [PubMed: 19374486]
15. Ashley RA, Roth CC, Palmer BW, Kibar Y, Routh JC, Fung KM, Frimberger D, Lin HK, Kropp BP. Regional variations in small intestinal submucosa evoke differences in inflammation with subsequent impact on tissue regeneration in the rat bladder augmentation model. BJU Int. 2010; 105(10):1462–1468. [PubMed: 19863527]
16. Tateya T, Tateya I, Sohn JH, Bless DM. Histological study of acute vocal fold injury in a rat model. Ann Otol Rhinol Laryngol. 2006; 115(4):285–292. [PubMed: 16676825]
17. Oksala O, Salo T, Tammi R, Hakkinen L, Jalkanen M, Inki P, Larjava H. Expression of proteoglycans and hyaluronan during wound healing. J Histochem Cytochem. 1995; 43(2):125–135. [PubMed: 7529785]
18. Molander N, Lindquist U, Stenevi U, von Malmborg A, Ehinger B. Influence of radial keratotomy on endogenous hyaluronan in cornea and aqueous humour. Refract Corneal Surg. 1993; 9(5):358–365. [PubMed: 8241040]
19. Kobayashi H, Terao T. Hyaluronic acid-specific regulation of cytokines by human uterine fibroblasts. Am J Physiol. 1997; 273(4 Pt 1):C1151–C1159. [PubMed: 9357758]
20. Wisniewski HG, Hua JC, Poppers DM, Naime D, Vilcek J, Cronstein BN. TNF/IL-1-inducible protein TSG-6 potentiates plasmin inhibition by inter-α-inhibitor and exerts a strong anti-inflammatory effect in vivo. J Immunol. 1996; 156(4):1609–1615. [PubMed: 8568267]
21. Toole BP. Hyaluronan in morphogenesis. J Intern Med. 1997; 242(1):35–40. [PubMed: 9260564]
22. Alho AM, Underhill CB. The hyaluronate receptor is preferentially expressed on proliferating epithelial cells. J Cell Biol. 1989; 108(4):1557–1565. [PubMed: 2466850]
23. Maytin EV, Chung HH, Seetharaman VM. Hyaluronan participates in the epidermal response to disruption of the permeability barrier in vivo. Am J Pathol. 2004; 165(4):1331–1341. [PubMed: 15466397]
24. Roth CC, Bell CH, Woodson B, Schultz AD, Palmer BW, Frimberger D, Fung KM, Lin HK, Kropp BP. Temporal differentiation and maturation of regenerated rat urothelium. BJU Int. 2009; 103(6):836–841. [PubMed: 19021621]

25. Witt M, Kasper M. Immunohistochemical distribution of CD44 and some of its isoforms during human taste bud development. Histochem Cell Biol. 1998; 110(1):95–103. [PubMed: 9681695]
26. Bourguignon LY, Ramez M, Gilad E, Singleton PA, Man MQ, Crumrine DA, Elias PM, Feingold KR. Hyaluronan-CD44 interaction stimulates keratinocyte differentiation, lamellar body formation/secretion, and permeability barrier homeostasis. J Invest Dermatol. 2006; 126(6):1356–1365. [PubMed: 16557236]
27. Kaya G, Rodriguez I, Jorcano JL, Vassalli P, Stamenkovic I. Selective suppression of CD44 in keratinocytes of mice bearing an antisense CD44 transgene driven by a tissue-specific promoter disrupts hyaluronate metabolism in the skin and impairs keratinocyte proliferation. Genes Dev. 1997; 11(8):996–1007. [PubMed: 9136928]
28. Wang C, Thor AD, Moore DH 2nd, Zhao Y, Kerschmann R, Stern R, Watson PH, Turley EA. The overexpression of RHAMM, a hyaluronan-binding protein that regulates ras signaling, correlates with overexpression of mitogen-activated protein kinase and is a significant parameter in breast cancer progression. Clin Cancer Res. 1998; 4(3):567–576. [PubMed: 9533523]
29. Brown AL, Srokowski EM, Shu XZ, Prestwich GD, Woodhouse KA. Development of a model bladder extracellular matrix combining disulfide cross-linked hyaluronan with decellularized bladder tissue. Macromol Biosci. 2006; 6(8):648–657. [PubMed: 16881043]

ABBREVIATIONS

CD44	cluster of differentiation 44
ECM	extracellular matrix
HA	hyaluronic acid
HABP	hyalyronan binding protein
HARE	hyaluronan receptor for endocytosis
LYVE-1	lymphatic vessel endothelial receptor 1
RHAMM	receptor for hyaluronan mediated motility
SIS	small intestinal submucosa

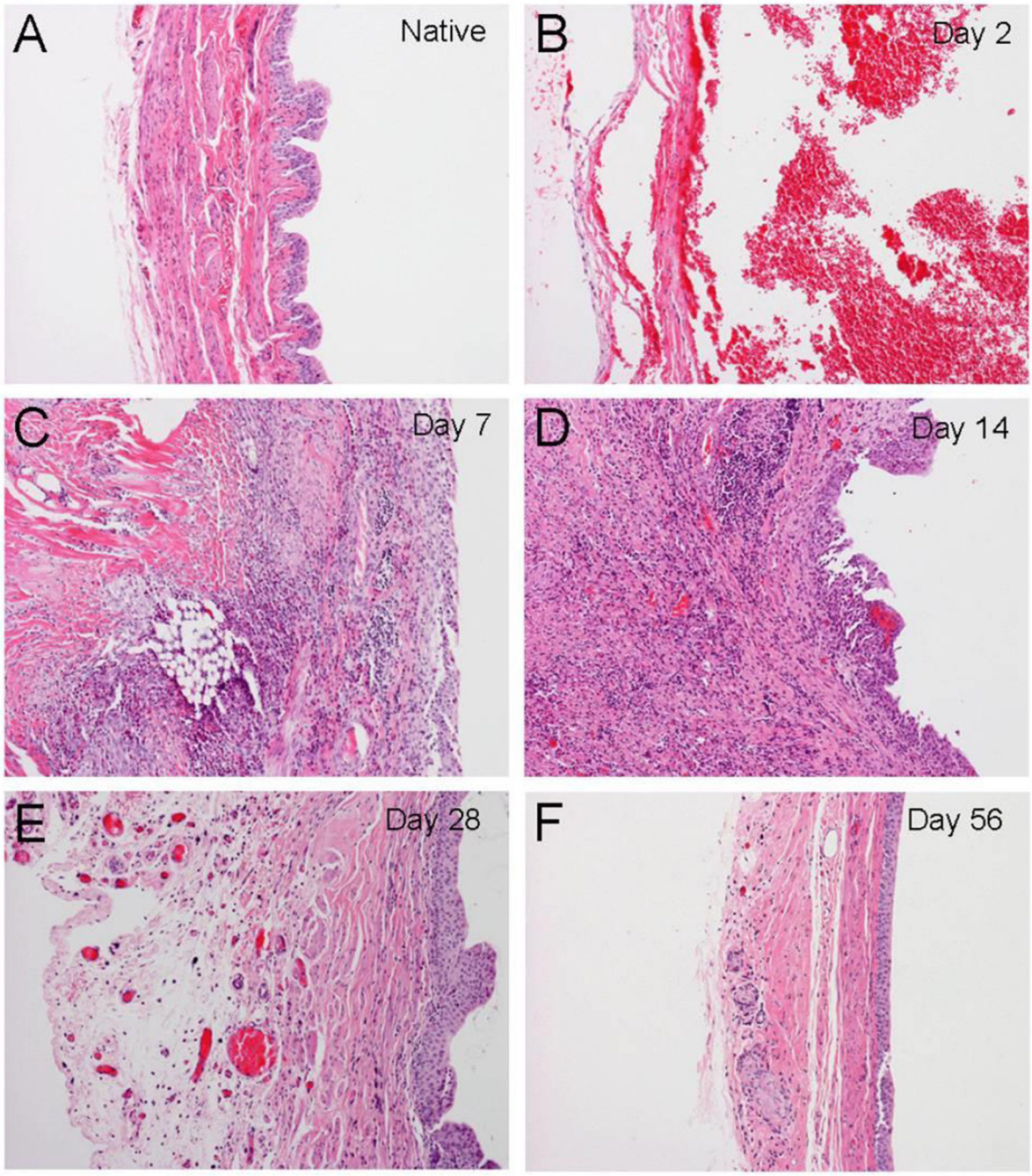

Figure 1. Histological presentation of regenerating rat bladders following SIS augmentation

Morphology is presented using H&E staining. (A) Normal rat bladder. (B–F) SIS-augmented bladders were harvested on days 2, 7, 14, 28 and 56 post-operation. Notice that the suture materials (arrow heads) are identified and confirmed regions of SIS grafts. Urothelial covering is almost complete by day 14. There is inflammatory cell infiltration in response to the surgery (small blue cells identified by the thin arrow); but the inflammation is largely resolved by day 28. Regenerating smooth muscle fibers can be identified in the

regenerating site (thick arrows). Note that giant cell granuloma in response to the suture material can be located in SIS graft areas. (Original magnification: 10× in all panels)

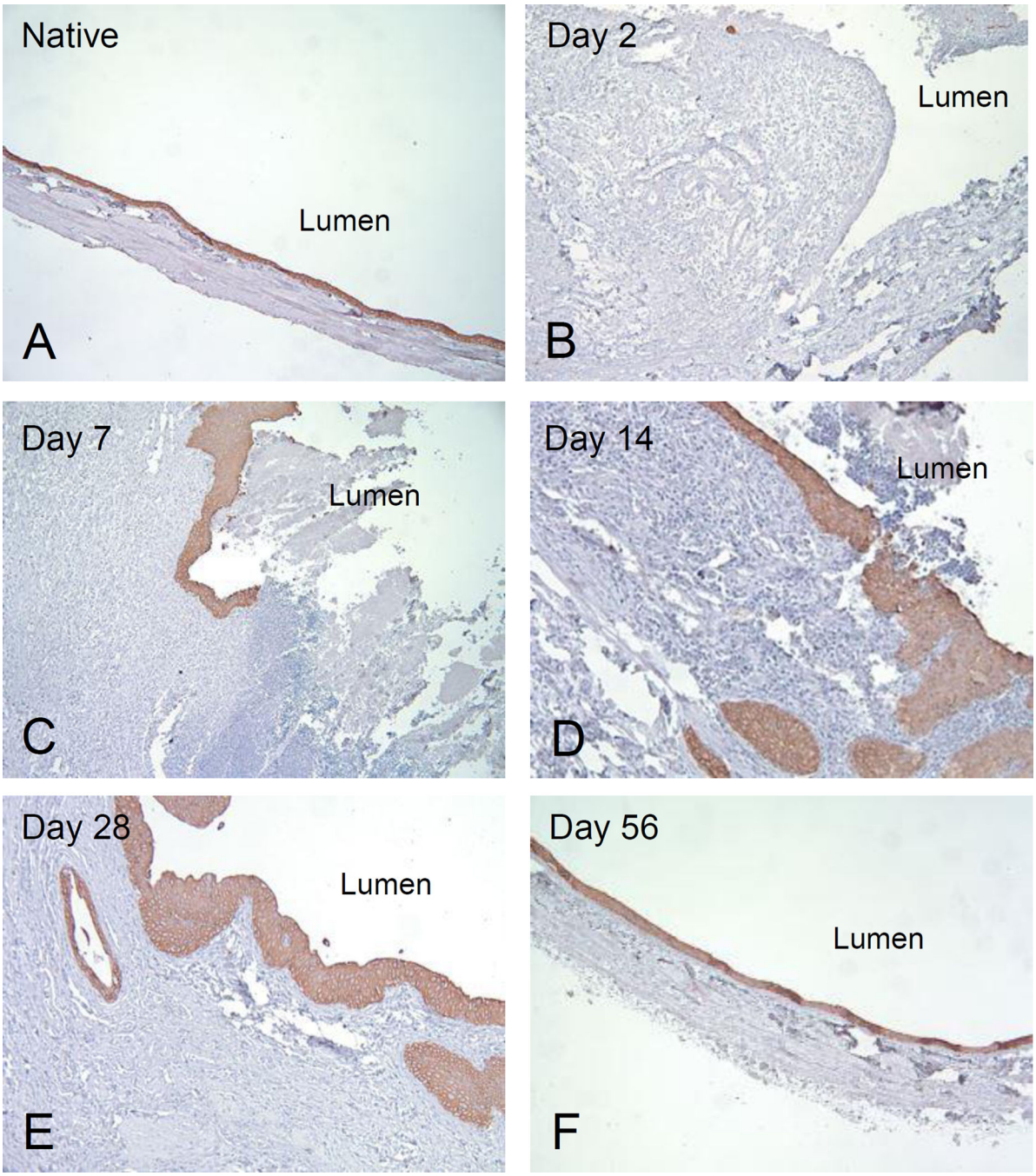

Figure 2. Re-epithelialization of regenerating rat bladders

Cytokeratin AE1/AE3 immunostaining was applied to identify the re-growth of the urothelium. (A) Normal rat bladder. (B–F) Re-epithelialization of SIS-augmented rat bladders between post-operatives days 2 and 56. AE1/AE3-positive staining is correlated with the appearance of epithelial cells from days 7 to 56 following augmentation. (Original magnification: 10× in all panels)

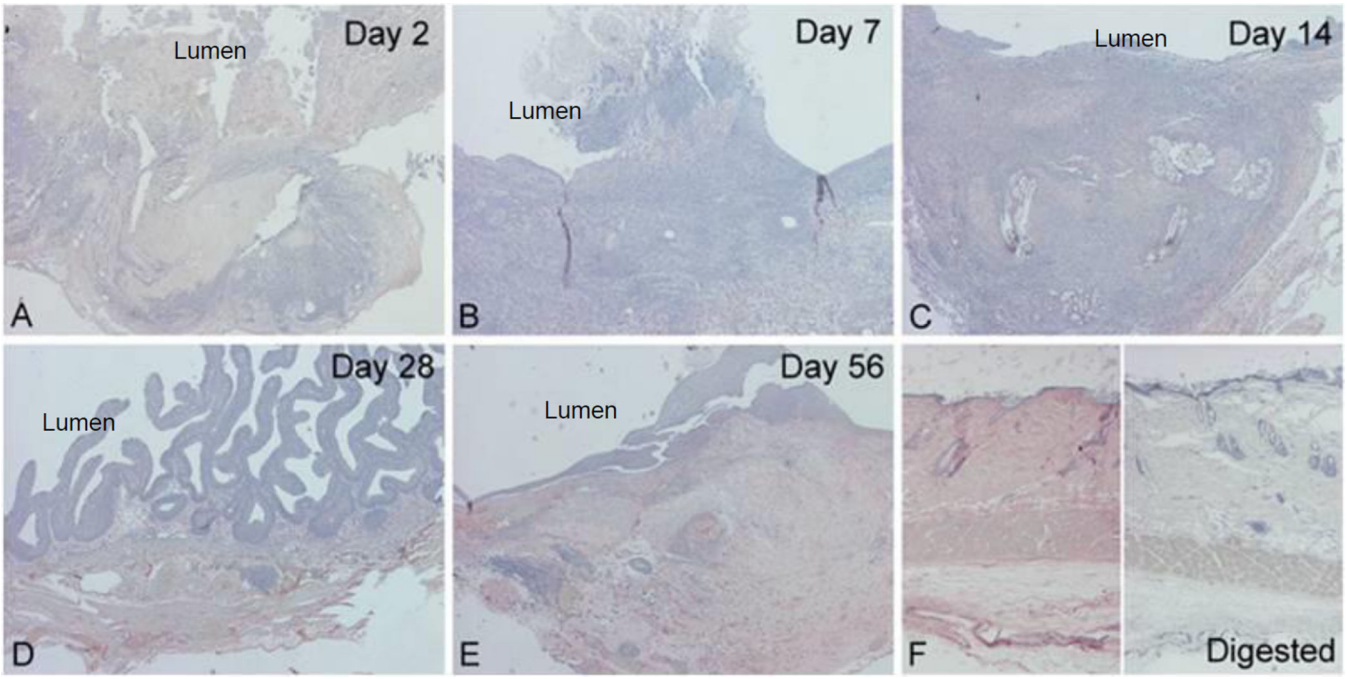

Figure 3. Immunohistochemical-like staining for HA in SIS-augmented rat bladders

HA deposition was determined by binding of HABP. (A–E) Immunoreactivity of HABP was determined between days 2 and 56 post-augmentation in SIS graft sections of regenerating bladders. The lumen of the bladder is indicated. (F) Rat skin was stained in parallel and used as a positive control. Tissue section digested with hyalurodinase was included as a negative control. The expression of HA in ECM is evident in red. The images were taken so that the urothelial cells are oriented upward. (Original magnification: 4× in all panels)

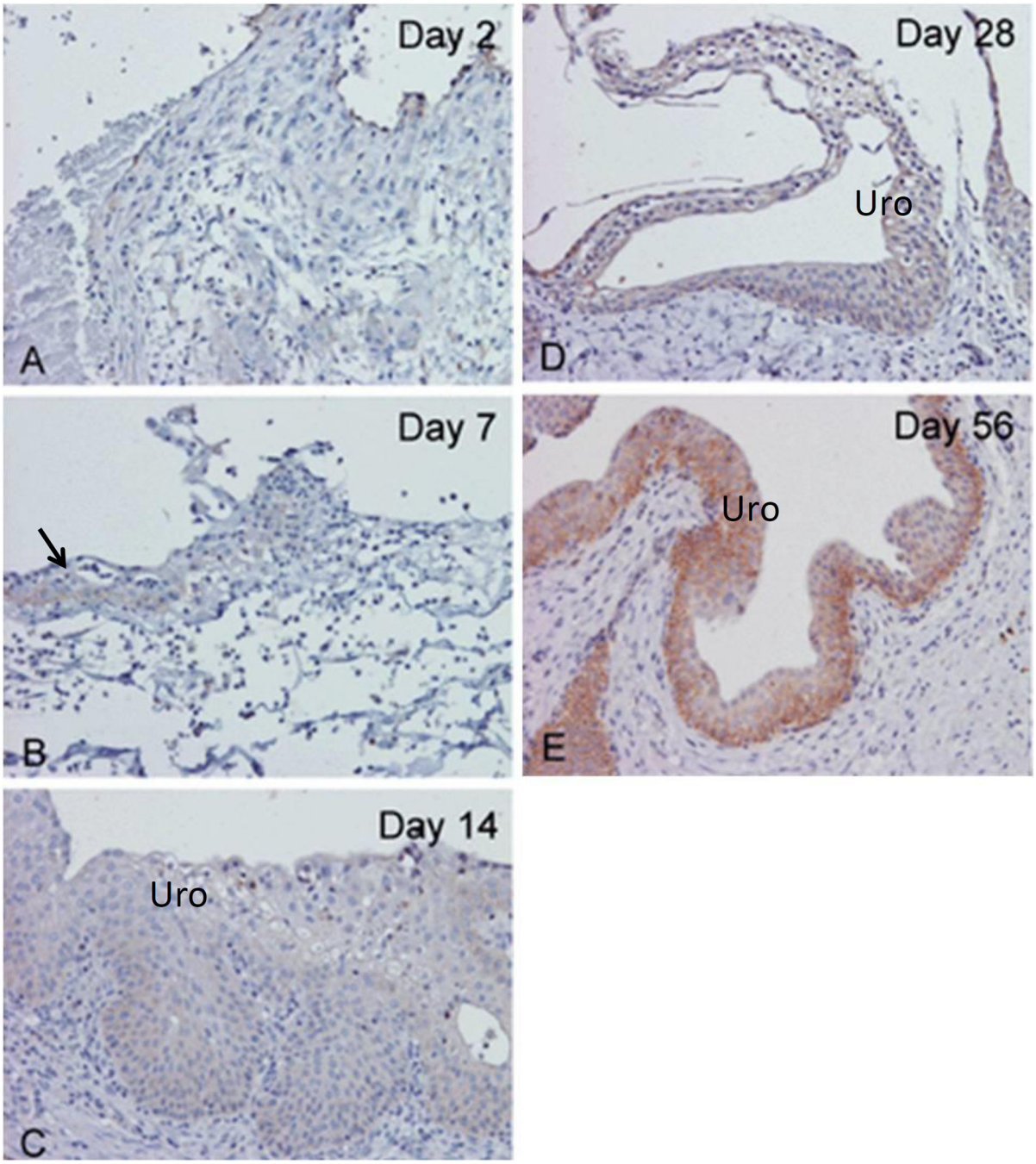

Figure 4. Immunohistochemical staining for CD44 in SIS-augmented rat bladders

(A–E) CD44 immunoreactivity was determined on post-operative days 2–56. CD44-positive immunoreactivity is mainly located in urothelium; and staining intensity increased as urothelial cell differentiated. (B) On day 7, only a small amount of regenerating urothelium is present (arrow). (C–F) A gradual increase in the immunoreactivity for CD44 is noted in the urothelium (uro) from days 14 to 56. (Original magnification: 20×)

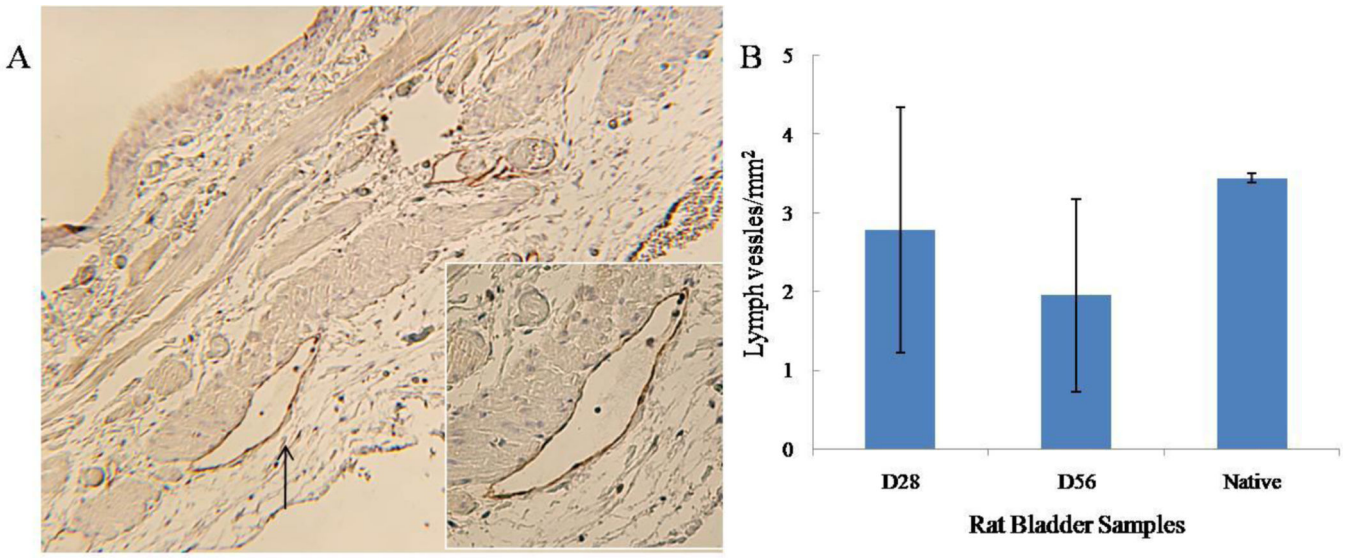

Figure 5. LYVE-1 immunoreactivity in SIS-augmented rat bladders

Immunohistochemical staining of regenerating bladders on post-operative days 28 and 56 are presented in panels A and B represent respectively. The expression of LYVE-1 in the lymph vessels is evident. The endothelial cells of lymphoatic vessels (arrow) are immunoreactive; but the endothelial cells of blood vessels are non-reactive. Red blood cells are indicated by the arrow. (Original magnification: 40×)

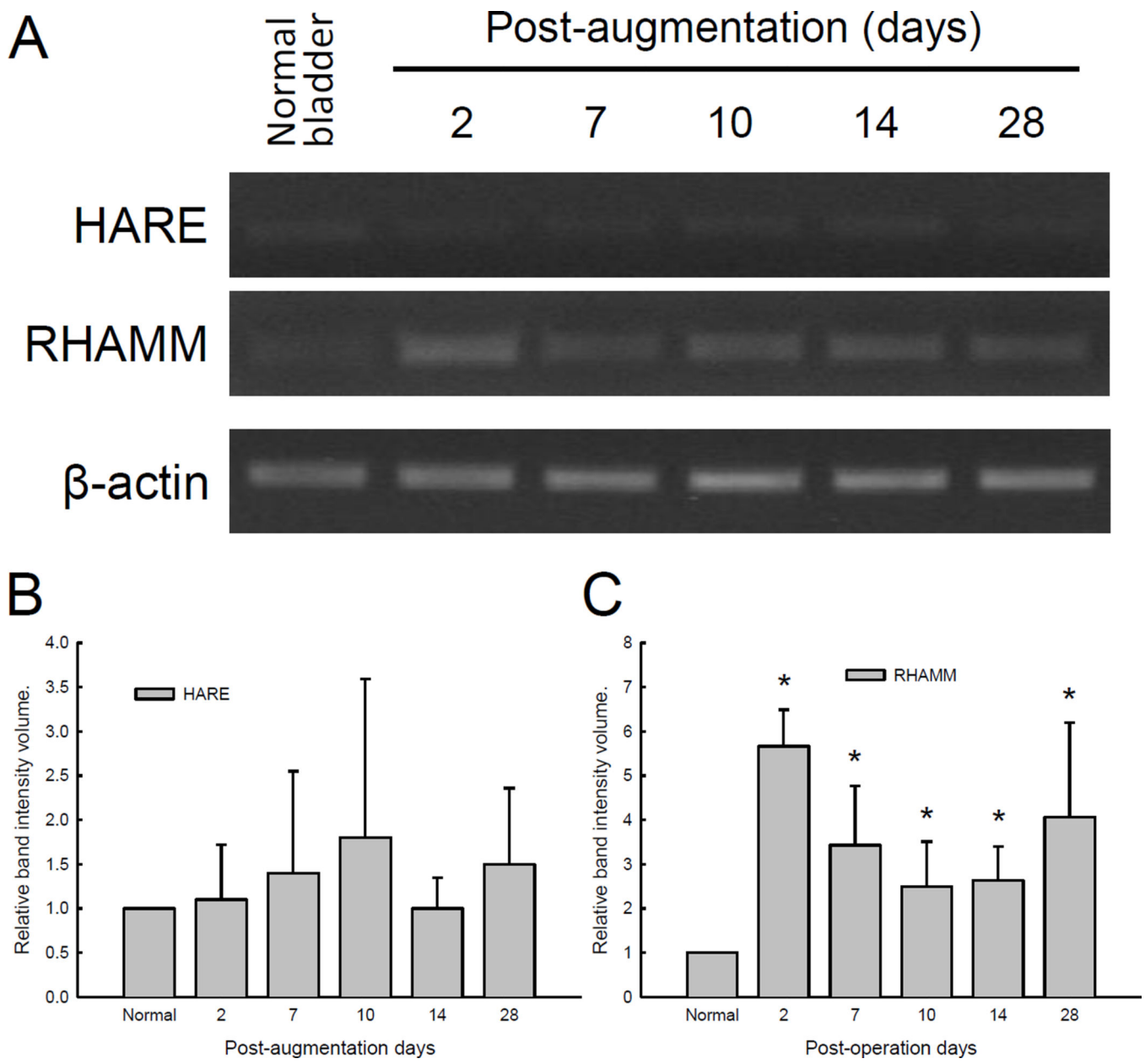

Figure 6. Expression of HARE and RHAMM mRNA in SIS-augmented rat bladders

A semi-quantitative RT-PCR method was applied to determine levels of HARE and RHAMM transcripts expression in SIS grafts between post-operative days 2 and 28. Bladder specimens harvested at the time of partial cystectomy were used as normal control. (A) Representation results of RT-PCR amplified HARE, RHAMM, and β-actin. (B–C) Semi-quantitative presentation of band intensities for HARE and RHAMM after normalization to β-actin and normal control bladders. * indicates statistical differences between regenerating and normal bladders ($p < 0.05$).